Probing Potential Energy Surface Exploration Strategies for Complex Systems

Gawonou Kokou N'Tsouaglo,[*,†] Laurent Karim Béland,[†] Jean-François Joly,[†] Peter Brommer,[‡] Normand Mousseau,[*,†,§] and Pascal Pochet[¶,‖]

[†]Département de physique and Regroupement québécois sur les matériaux de pointe, Université de Montréal, C.P. 6128, Succursale Centre-Ville, Montréal, H3C 3J7 Québec Canada

[‡]Centre for Predictive Modelling, School of Engineering, University of Warwick, Coventry CV4 7AL, United Kingdom

[¶]Université de Grenoble Alpes, INAC-SP2M, L_Sim, F-38000 Grenoble, France

[§]Laboratoire de Physique Théorique de la Matière Condensée, Université Pierre et Marie Curie, Boite 121, 4, Place Jussieu, 75252 Paris Cedex 05, France

[‖]CEA, INAC-SP2M, Atomistic Simulation Laboratory, F-38000 Grenoble, France

Ⓢ *Supporting Information*

ABSTRACT: The efficiency of minimum-energy configuration searching algorithms is closely linked to the energy landscape structure of complex systems, yet these algorithms often include a number of steps of which the effect is not always clear. Decoupling these steps and their impacts can allow us to better understand both their role and the nature of complex energy landscape. Here, we consider a family of minimum-energy algorithms based, directly or indirectly, on the well-known Bell–Evans–Polanyi (BEP) principle. Comparing trajectories generated with BEP-based algorithms to kinetically correct off-lattice kinetic Monte Carlo schemes allow us to confirm that the BEP principle does not hold for complex systems since forward and reverse energy barriers are completely uncorrelated. As would be expected, following the lowest available energy barrier leads to rapid trapping. This is why BEP-based methods require also a direct handling of visited basins or barriers. Comparing the efficiency of these methods with a thermodynamical handling of low-energy barriers, we show that most of the efficiency of the BEP-like methods lie first and foremost in the basin management rather than in the BEP-like step.
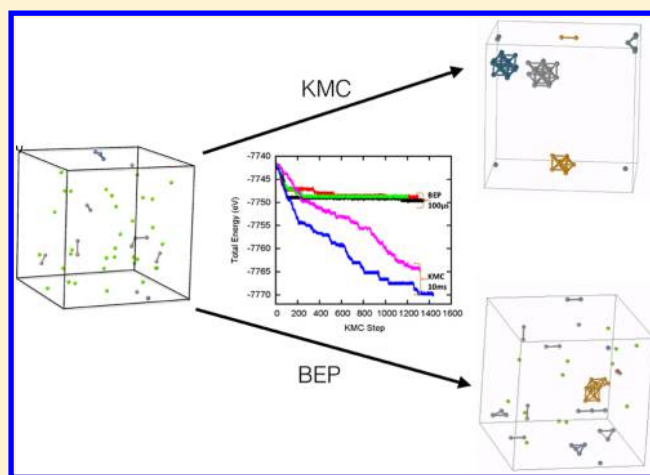
1. INTRODUCTION

Finding pathways toward global minima on the energy landscape of complex materials is a major challenge in many fields.[1] In the last decades, we have observed the multiplication of new approaches for accelerating the exploration of the energy landscape space while still attempting to follow physically-relevant pathways (see, for example, refs 2–6).

Because the complexity of energy landscapes increases at least exponentially with system size,[7,8] many efforts have gone into identifying local features that could be used to bias the search toward global low-energy structures. Such knowledge would allow one to generate physically relevant and efficient moves much more quickly, reducing the size of the effective landscape and increasing the probability of constructing pathways leading to global energy minima.

Among the various propositions, a number of groups have suggested, either directly or indirectly, that the Bell–Evans–Polanyi (BEP) principle,[9–11] developed in physical chemistry, could also apply to more complex systems.[5,7,12,13] The BEP principle states that the lowest-energy barriers surrounding a local minimum lead to deeper low-energy states; following systematically the lowest-energy barrier out of a local minimum should therefore rapidly lead to deep minima. It is closely connected to the methods that follow the lowest vibrational normal mode(s) to establish folding pathways and find native states of proteins and other molecules.[14] While the BEP principle has been used mostly for molecules,[15] its application to bulk matter is relatively new.[5,12]

Indeed, a simple application of the BEP principle inevitably leads to trapping since the trajectory is fully determined by the local structure of the energy landscape: once at the bottom of a local energy basin, the BEP principle does not allow any escape route into a new basin. This is why recently proposed

algorithms have coupled the BEP approach to basin-handling algorithms that force the system out of local basins, ensuring a more complete sampling of the landscape. In fact, most energy landscape exploration methods include generally an additional step for handling flickers, i.e. nondiffusive states separated by low-energy barriers that increase the energy landscape complexity without contributing to the system evolution, and frequently visited states. A number of approaches have been proposed for handling these states, including the exact treatment of their kinetics[6,16−20] and Tabu-like methods, approaches that block already visited states or transitions, facilitating the overall phase-space sampling.[21−24]

Because of BEP's simplicity and its fundamental relation to energy landscape, it is useful to try to disentangle the contribution of the various elements composing recently proposed BEP-based algorithms such as the autonomous basin climbing (ABC)[13] and the minima-hopping[5] methods. In this article, we assess these methods by comparing their application with kinetic Monte Carlo (KMC), an algorithm known to provide the correct kinetics.[25] This comparison allows us to better understand how these methods work and, more importantly, what the nature of the energy landscape of complex bulk systems is. To do so, we use the kinetic Activation-Relaxation Technique (k-ART), an off-lattice KMC method with on-the-fly catalog building, that handles both disordered systems and long-ranges deformations directly as the reference simulation package, since it provides physically accurate trajectories with which to compare the efficiency of the BEP-based exploration algorithms.[6,23]

In the following section we describe the implementation of the various methods. We then present results from tests run on two systems: vacancy aggregation in iron and relaxation of an ion-implanted box of crystalline silicon. The significance of these results is presented in the discussion section. When handling flicker states correctly, we find that crossing high-energy barriers is essential to open new low-energy pathways, by moving into unvisited energy basins that can lead to new low-energy structures. On the other hand, while Tabu does not preserve the correct kinetics, it significantly raises the efficiency of BEP but does not significantly accelerate the configurational space sampling as compared with standard KMC with flicker-handling.

2. METHODOLOGY

The comparison presented in this paper is done, first, between two sampling algorithms, kinetic Monte Carlo and the BEP principle. For each of these methods, we apply two different approaches for handling low-energy barriers. All these are run using the kinetic Activation-Relaxation Technique (k-ART) package as a base.[6,23] In this section, we first describe the k-ART package and then each algorithm separately.

2.1. The Kinetic Activation-Relaxation Technique. The kinetic Activation-Relaxation Technique (k-ART) is an off-lattice kinetic Monte Carlo algorithm (KMC)[25] that lifts many of the technical restrictions preventing its application to complex materials.[6,23] Traditionally, KMC uses a fixed, preconstructed event catalog to compute the rate of escape from a local minimum and brings forward the simulation clock according to a Poisson distribution.[25,26] This choice limits the atomic motion to discrete states, which are generally crystalline positions, preventing its application to disordered or defective materials, alloys, and, in many cases, semiconductors and

leaving aside much of the long-range elastic effects on energy barriers and kinetics.

While k-ART is described in detail in refs 6, 27, and 28, it is useful to provide here a short description of the algorithm. Updating the system in k-ART can be described as a four-step process:

1. After a move, all atoms are inspected for changes in local environment. A spherical region around each atom, with a radius typically set to between 5 and 7 Å, is defined. A bonding graph is constructed between atoms within this region, by connecting nearby atoms within a preset cutoff, generally fixed between the first and second neighbor. Using NAUTY,[29] a topological analysis library, we identify the unique automorphic group associated with this bonding graph, irrespective of the various symmetry operations. This allows us to construct a discrete and reusable catalog even for totally disordered systems.

2. For each new topology encountered, excluding the crystalline ones that would only lead to improbable events on the simulation time scale, we launch a series of event searches using the latest version of ART nouveau.[30,31] For the two systems studied here, we launch 50 random event searches for each new topology and restrict our search to events with an energy barrier less than or equal to 5 eV, generating on average between 3 and 5 events per topology and therefore per atom in a nonperfectly crystalline environment. To ensure a complete catalog, new searches are also regularly launched on the most common topologies.

3. Once the catalog is updated to include events associated with the new topologies, all events corresponding to the current configuration are placed in a binary tree in preparation for the KMC step. All barriers corresponding to at least 99.99% of the rate, computed with constant prefactor, are then reconstructed and fully relaxed to account for geometrical rearrangements due to short- and long-range elastic deformations. The final individual and global rates are therefore associated with the exact conformation.

4. Finally, the standard KMC algorithm is applied to select an event to execute it and advance the clock according to a Poisson distribution. Once the event is executed, we return to (1) for the next step.

Using topological classification coupled with an unbiased open search for transition states, k-ART handles events without regard to the presence or not of a crystalline substructure, constructing the event-catalog as the system evolves and fully taking care of all elastic effects. Parallelizing event searches over tens to hundreds of processors,[6,27] k-ART has been applied with success to highly defective crystals,[32−35] alloys, and even amorphous materials,[36] generating atomistic trajectories on time scale of 1 s or more and providing insight in the long-time dynamics of these systems.

2.2. Implementing the Bell−Evans−Polanyi Principle. The Bell−Evans−Polanyi (BEP) principle is based on the observation that the local curvature on the energy landscape is almost constant for given systems.[12] Taken to its extreme (see Figure 1), BEP implies that the barrier height out of a local minimum is a direct indicator of the depth of the following energy minimum so that, to obtain the maximum relaxation in a single step, one should select the lowest available energy-barrier.

Implementing the Bell−Evans−Polanyi principle is straightforward within k-ART. We follow steps (1) to (3) according to the description above. The only difference is that after all
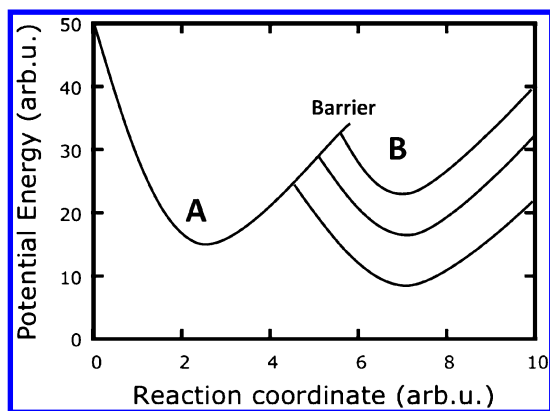
Figure 1. Bell−Evans principle: if all local-energy basins are similar in size, then selecting the lowest-energy barrier from an initial minimum (A) will lead to the lowest-energy minimun in (B) and an overall faster energy relaxation.

barriers have been relaxed, the lowest-energy barrier is systematically selected within the limits of the flicker handling method as discussed in the next subsection. Although time has no physical meaning with the BEP approach, we still use the KMC rate to assign a clock to the BEP evolution for comparison with k-ART results.

2.3. Handling Flickers. The efficiency of event-based simulations is limited by the presence of flickers, nondiffusive states of similar energy separated by a low-energy barrier with respect to those leading to structural evolution. When the KMC or BEP strategy, as defined above, is applied to any system with more than a few barriers, simulations become trapped rapidly within flickers that seize all computational efforts without structural evolution. Many efforts have gone into handling flickers since KMC was first introduced to material sciences, 25 years ago.[25] Here we consider two approaches: the basin autoconstructing Mean-Rate Method (bac-MRM),[6] that we have adapted from Puchala et al.'s Mean-Rate Method,[18] and a simple barrier-based Tabu.[21−23]

The bac-MRM, discussed in detail in ref 6, handles flickers by merging the associated states within a single basin, solving the internal dynamics analytically, projecting the solution onto the various exit pathways, and correcting their respective rate. Since the bac-MRM is statistically exact and since by definition the in-basin states have very close energy, it is possible to adjust the basin barrier cutoff as the simulation evolves to prevent it from being trapped.

When the focus is on sampling configurations rather than following the right kinetics, it is possible to limit or even forbid the visit of already known states. In barrier-based Tabu, when a barrier is selected, we compare the trajectory, i.e. the displacement from the initial to saddle to final state, with the last N moves (see ref 22 for more details). If the displacement is not in the database, the event is generated, otherwise, the configuration is left in the initial or final state according to their respective Boltzmann weight. The transition can be completely forbidden for the rest of the simulation or blocked for a number n of steps, hence the name *Tabu*. Here we select $n = 50$.

2.4. Links to Other Algorithms. K-ART simulations apply the kinetic Monte Carlo algorithm coupled with the bac-MRM, which offers a statistically correct kinetics.[6] Methods such as the autonomous basin climbing[13] and the minima-hoping[5] minimization algorithms, for their part, generate trajectories that go over the lowest-available energy barrier separating two

energy basis, following BEP. To avoid getting trapped into local minima, both of these methods implement Tabu-like algorithms to prevent revisiting the same minima over and over again. More precisely, ABC adds a bias potential to the visited states, while minima-hopping increases the kinetic energy of the MD pulses when previously found states are revisited.

If the implementation details for the various BEP-based algorithms differ, the effect is very similar: states are never formally blocked with either ABC or minima-hoping approaches, but the bias potential and the MD pulse do not impose any formal upper limit to the energy barrier that can be crossed when the system is trapped in a local basin. The resulting escape is therefore very close to Tabu and differs fundamentally from flicker-handling methods, such as bac-MRM, that keep an energy threshold that guarantees the correct kinetics (see Figure 2 for a cartoon picture).
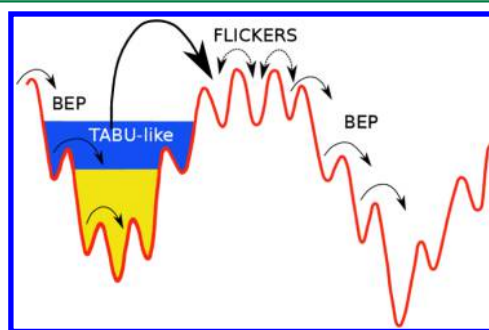
Figure 2. A model of energy landscape of complex material with a number a deep energy basins as well a flickering states that are sampled with BEP and Tabu-like methods.

The simplified implementation of the various BEP-like algorithms that is used here allows us, therefore, to identify more clearly the role of the various elements found in the published methods.

2.5. Systems Studied. We compare the KMC and BEP methods and the impact of flicker handling on two different systems: (1) the aggregation of 50 vacancies inside a 2000-atom box of bcc iron described with the Ackland potential[37] and (2) the relaxation of a 27000-atom box of c-Si disordered through the implantation of a single 3-keV Si ion and described with the Stillinger-Weber potential.[38] Both systems are run at 300 K and at constant volume corresponding to crystalline density.

For the iron system, we start with a 2000-atom bcc Fe cubic box and remove 50 atoms at random. Both BEP and KMC simulations are launched after a simple local energy minimization. For the Ackland potential, the vacancy diffusion barrier is found to be 0.64 eV with MD[37] and ART nouveau. At 300 K, aggregation from random vacancies into 9 to 10 vacancy clusters was found to take on the order of 1 ms in three independent off-lattice KMC simulations.[32,39,40]

The initial configuration of ion-implanted Si is described in detail in ref 33. A 3-keV ion is first implanted in a 100 000-atom Stillinger-Weber box[38] with two surfaces along the z-direction and periodic boundary condition (PBC) along the x and y directions and is then relaxed for 10 ns using NVT molecular dynamics at 300 K. A block of 27 000 atoms surrounding the disordered region is then extracted and placed into a cubic cell with PBC along the three axes. The kinetics of relaxation with

k-ART and bac-MRM was found to be in excellent agreement with nanocalorimetric measurements.[33,34]

3. RESULTS

3.1. Basin Mean Rate Method. We first compare the k-ART and BEP relaxation methods coupled with the bac-MRM using the Fe system. For the initial state of a 2000-atom bcc-iron box see the Supporting Information. We run three independent simulations for BEP and two for KMC. Each run is about 1300 k-ART steps not counting flickering steps that are handled with the bac-MRM. Figure 3 reports the evolution of the total energy as a function of KMC step and as a function of time, respectively.
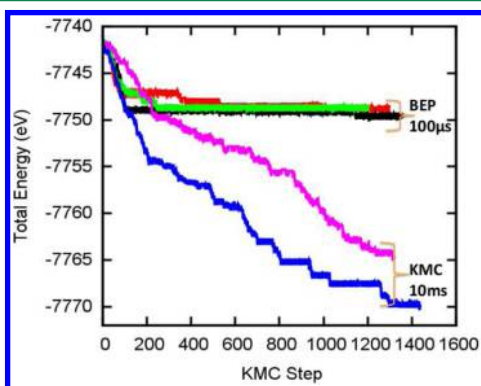
Figure 3. Evolution of the potential energy for three BEP and two KMC runs of the 50-vacancy FE system as a function of simulation step.

The five simulations, using either k-ART or BEP, follow a similar trajectory for the first 100 steps or so. At that point, all BEP simulations are trapped at an energy about 7 eV below the initial configuration for the rest of the simulations (more than 1000 steps further for each run), unable to find pathways to more relaxed states, while the KMC simulations evolve the system for the whole run, finishing between 25 and 28 eV below the BEP runs. Projecting these runs on a time axis, we see that the two methods follow the same path until about 10 μs, at which point the clock for BEP runs slows down noticeably compared to KMC: after 1300 steps, BEP runs reach about 100 μs compared with 1 to 10 ms for KMC.

This difference in effective time is not caused by the handling of flickers, since both k-ART and BEP use, here, the bac-MRM. Indeed, these BEP simulation results are consistent with Fan et al.[41] recent work using the Autonomous Basin Climbing (ABC) method, a BEP-like approach.[13] Using the same 50-vacancies Fe system, ABC simulations produced an energy drop of 13 eV during a simulation lasting 20 000 s, while k-ART reaches the same energy level in the first 500 μs of simulation and continues to relax well-below ABC's level. Figure 4 compares the performance of k-ART with KMC with that of Autonomous Basin Climbing (ABC) for this system.

To understand the difference between these two methods, we look at the time evolution of the average vacancy cluster and the monovacancy fraction for one BEP and KMC simulation (Figure 5 (a)). These correspond respectively to the green and blue lines in Figure 3. As for the energy, structural evolution for the two simulation types follows a similar path for the first 10 μs, which corresponds to the clustering of about 38% of the initial value of the vacancies into small clusters (averaged
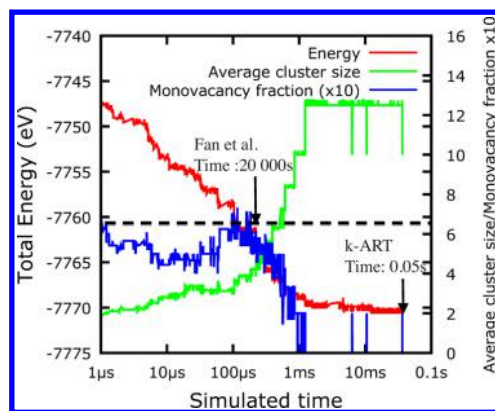
Figure 4. Comparison of k-ART vs ABC relaxation for the Fe system. Red line: total energy evolution as a function of logarithmic of simulated time; green line: evolution of cluster size; blue line: evolution of the fraction of monovacancies. The horizontal dashed black line corresponds to the energy level reached after 20 000 s with ABC.
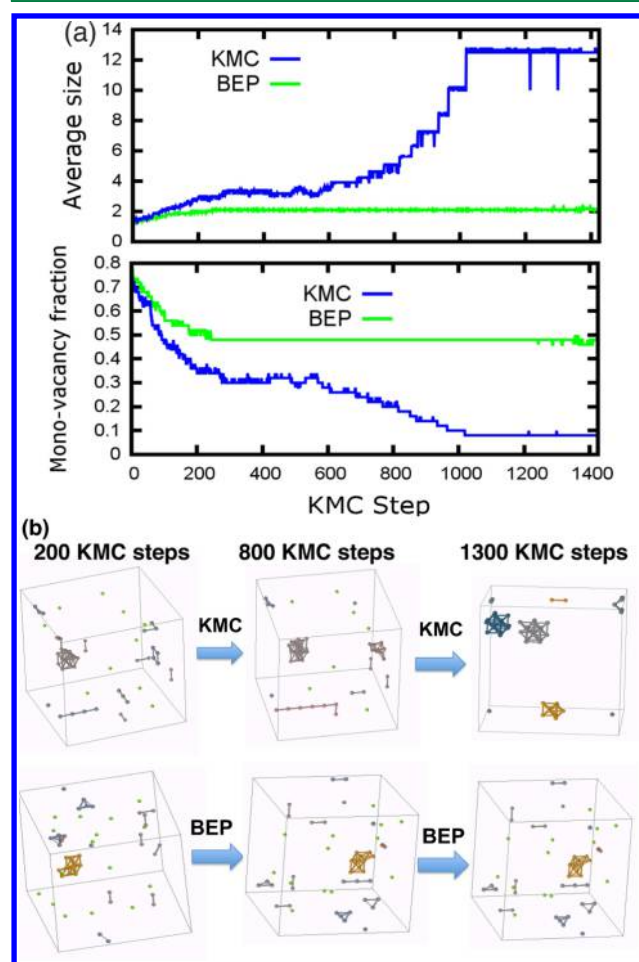
Figure 5. (a) Comparison of k-ART vs BEP for structural evolution for the Fe system. Top: Evolution of the average cluster size as a function of simulation step. Bottom: Evolution of the fraction of monovacancies. Blue line: KMC; green line: BEP. (b) Selected snapshots of the atomic configuration for a KMC and BEP runs at 200, 800, and 1300 simulations steps. Only vacancies are shown. Colors are associated with cluster size. Monovacancies are colored in green, cluster containing two vacancies are colored in gray, and trivacancies are colored in dark.

cluster size equals two). At that stage, the structural evolution of the BEP run comes almost to a stop, while the aggregation continues with KMC simulation with clusters reaching an average size of 13 as the proportion of monovacancies falls to less than 12.5% of the initial value. This supports the relation between BEP and Fan et al. simulation observed for the total energy (blue line in Figure 4), where the monovacancy fraction decreased to only 52% of the initial value (averaged size 6) after 20 000 s. The structural difference between the final BEP and KMC states is clearly seen in the snapshots taken during the evolution of both simulation types (Figure 5(b)). Even at 800 simulations steps, we note a difference in the number of isolated vacancies between the two types of runs.

To further understand the kinetic evolution of these two simulations sets and their relation to the structure of the energy landscape, we analyze the evolution of the energy barrier height for all *executed* events. Figure 6 (top) shows all the energy
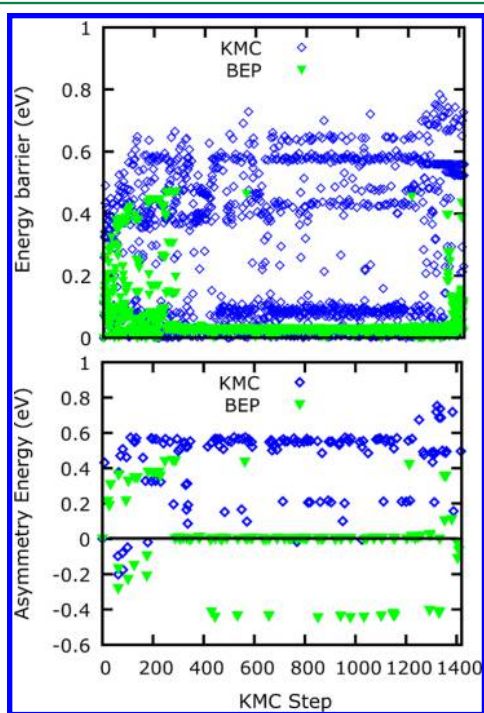
Figure 6. Top: Distribution of the executed energy barriers as a function of the simulation step step for both BEP (green triangle) and KMC (blue squares) simulations of the Fe 50-vacancy system. Bottom: Asymmetric energy, i.e. energy difference between the final and initial energy states, for events within the top highest 10% energy barrier as a function of simulation step in the same system.

barriers for executed events as a function of step of KMC and BEP simulations. For KMC simulations, we note that the maximum barrier height increases with the step, but that, in any step frame, the energy barrier distribution remains almost continuous. For BEP simulations we note instead, the maximum barrier height visited—around 0.4 eV — has been reached and that, after this point, the same distribution of barrier is selected until the simulations stopped after 1300 steps. KMC manages therefore to access activated barriers that are slightly higher, 0.5 eV, than those crossed with BEP but sufficient to unlock configurations by giving access to new relaxation pathways.

Why would crossing high barriers be so important? Figure 6 (bottom) plots the energy released by the system, or the

asymmetry energy, for executed events associated with the 10% highest energy barriers calculated in a moving window. In this plot, negative asymmetry energy means that the system has moved into a state of lower energy, while positive values are associated with higher energy final states. We see that 93% of these events lead to states with a higher final energy in KMC simulation versus 53% events in BEP simulation. In BEP, crossing these high energy barriers leads, almost half the time, to lower energy states and, as often, to higher energy states, while, for KMC runs, the bias is clearly toward higher energy states.

Before discussing the significance of this observation, we first need to check whether these results are seen in other systems.

To ascertain the generality of the results on Fe, we repeated the study on a disordered covalent system with an equal number of vacancies and interstitials: a 27 000-atom ion-implanted crystalline silicon. As shown in the Supporting Information, both systems provide similar overall results to the Fe system.

3.2. Tabu. We now look at the effect of Tabu, an approach that can be applied not only to handle flickers in kinetic simulations but also to orient relaxation when searching for global minimum. We compare Tabu with bac-MRM using both BEP and KMC sampling techniques. Figure 7 (a) shows the evolution of the total energy for a 2000-atom Fe box with 50 vacancies as a function of simulation step. We note that KMC-bac-MRM provides the fastest overall relaxation, reaching -7770 eV after 2250 steps, almost 80% faster than Tabu-KMC or BEP. Nevertheless, in the long run, Tabu, irrespective of the sampling method, manages to reach KMC-bac-MRM's relaxation level and even, in one simulation, achieve a better energy gain.

For large-scale complex system, Tabu becomes less efficient. Figure 7 (b) presents the total energy evolution as a function of the simulation step of a 27000-atom box of c-Si disordered through the implantation of a single 3-keV Si ion for two runs of BEP with Tabu and one run with bac-MRM, and two runs of KMC with Tabu and one run with bac-MRM. We see the two simulations using Tabu with BEP held at high energy state and Tabu with KMC simulation descending following the same pathway as with bac-MRM with KMC, due, in part, to the limited 50-step memory kernel used here.

Figure 8 gives the energy released for all *selected* events for one Tabu-BEP and one Tabu-KMC simulation for the top 10% highest executed energy barriers crossed calculated over a moving time window. Analysis of the energy barrier height evolution for these simulations shows that Tabu-based simulations display a similar rate of visiting higher final energy states as previously observed for KMC-bac-MRM: 84% of Tabu-KMC events and 93% Tabu-BEP events lead to higher energy states. This explains why Tabu approaches can be, on average, as efficient as KMC-bac-MRM for finding low-energy states. By blocking already visited directions, Tabu effectively forces the system to sample the more asymmetric states that lead to overall lower-energy configurations. This might explain also why, since minima-hopping uses a Tabu-like approach, by systematically increasing the exit energy, the method remains efficient even though it is based on the BEP principle.[5,12]

In spite of these similarities, it is important to remember that bac-MRM is statistically exact, contrary to Tabu, and that it preserves the correct dynamics of the system. For example, analysis of energy evolution for the four Tabu simulations
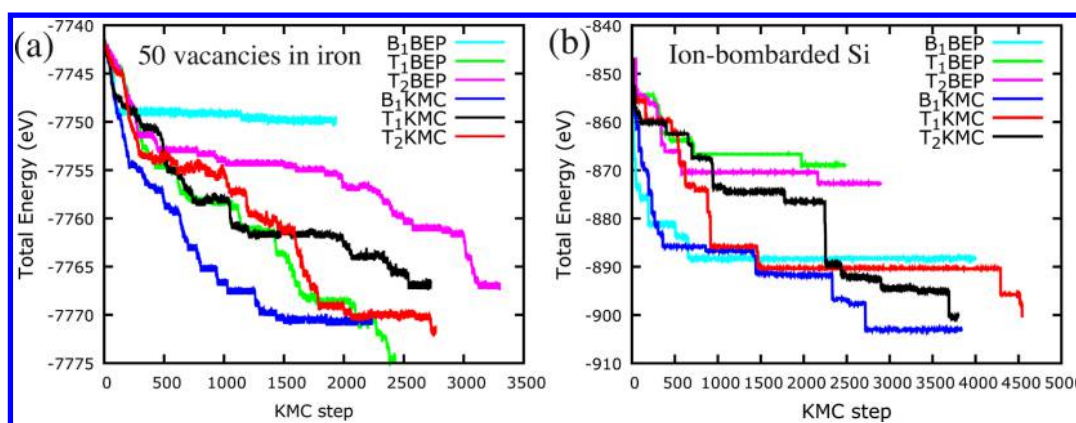
Figure 7. Evolution of the potential energy as a function of simulated step for various simulations. (a): (Fe vacancies system) BEP with bac-MRM (B_1BEP), two independent BEP runs with Tabu (T_1BEP and T_2BEP) and the same with KMC (B_1KMC, T_1KMC, and T_2KMC). (b): (Ion-implanted Si) BEP with Tabu and 1 run with bac-MRM, and 2 runs of KMC with Tabu and 1 run with bac-MRM.
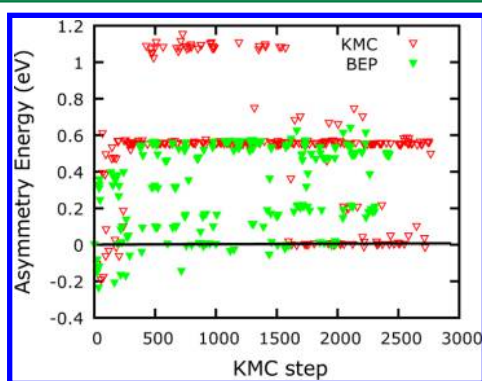
Figure 8. Asymmetric energy, i.e. energy difference between the final and initial energy states, for events within the top highest 10% energy barrier as a function of simulation step for the Tabu-based KMC and BEP simulations of the 50-vacancy Fe system.

shows sudden staircase-like decrease for the energy (Figure 7), a behavior that is not observed with the bac-MRM simulations.

4. DISCUSSION

These results allow us to better understand the applicability of the BEP principle to bulk systems, the importance of the flicker-handling methods as well as more about the structure of the energy landscapes.

As discussed in the Introduction, the BEP principle was formulated many decades ago, and it has helped to understand various kinetic phenomena in chemistry. In its simplest form, it states that around a given local energy minimum, the lowest energy-barrier will lead to the lowest energy state among those directly connected to the initial minimum. In a recent paper, Roy and collaborators showed that a relaxed version of BEP is applicable to bulk systems: crossing a small barrier has more chances to lead to a deep minimum than crossing a high-energy barrier.[12]

This observation is correct but incomplete. Extensive characterization of the energy landscape of amorphous silicon (a-Si), for example, has shown that in fact for any event the forward and reverse barrier height, i.e. the barrier height computed from the initial and the final minima, respectively, are totally uncorrelated.[42] This general observation also holds, at least, in ion-bombarded Si.[34] Since the depth of the final well, as measured from the initial state, is the difference between the reverse and the forward barrier height, this absence of

correlation means that, on average, lower forward energy barriers do lead to deeper minima, which explains some of the success of the application of the BEP principle to materials.[43,44] Fundamentally, therefore, the structure of the landscape does not correspond to the original BEP principle, which states that there is a direct correlation between the barrier height and the depth of the final minimum.

Since the BEP principle is correct locally on average, even though for the wrong reasons, is strictly following the lowest available energy barrier, with respect to the BEP principle, an efficient global minimization approach?

Results presented in the previous section show that it is not the case, as should be expected for complex materials. To relax efficiently, both the Fe vacancy and the ion-implanted Si systems require crossing barriers that do not correspond to the lowest ones available in order to land into higher energy states, a move that goes beyond BEP-based approaches. As was shown recently in ion-implanted c-Si and a-Si, accessing these high-energy states is essential to open new low-energy pathways, by moving into unvisited energy basins that can lead to low-energy structures.[33,36] This so-called *replenish and relax* mechanism explains why, when treating correctly the local flickering dynamics, BEP approaches cannot be as efficient as standard KMC methods. Clearly, systematically selected lower energy barriers are not sufficient to exit local energy basins.

Why then do BEP-based relaxation methods succeed in finding low-energy states? The crucial step is in the way the code handles local-energy traps. When applied to BEP runs, for example, Tabu manages to prevent the trajectories from getting trapped, allowing simulations to reach energy levels similar to those obtained with the KMC method, in a similar number of steps. This is done, essentially, by violating the BEP principle and systematically blocking the lowest energy barrier, allowing the system to cross over higher energy ones. Tabu, as was shown by Grebner et al.,[24] even enhances sampling of efficient search methods such as simulated annealing and Basin Hopping.[3]

These results confirm that efficient energy minimization in a bulk system cannot be based on the BEP principle alone for two reasons. (i) The BEP principle is not exact: it is the absence of correlation between the forward and backward energy barriers that explains why lower-energy barriers tend to lead to deeper energy minima, not a specific correlation between these two quantities. (ii) More important, complex

systems are composed of many minimum-energy basins; it is therefore necessary to go over higher-energy states in order to reach new deep-energy minima. This can be done either by using a physically based kinetic algorithm such as simple MD[45] or KMC or by systematically limiting the available phase space to nonvisited regions,[13,24] in effect forcing the system to move over these high-energy barriers.

These results allow us to better understand what the crucial elements explaining the efficiency of recently proposed BEP-based algorithms are. They also demonstrate that in out-of-equilibrium systems the odds of revisiting the same basin, when it does not correspond to the global minimum, is small. While, in this case, efficient sampling is helped by the capacity of selecting from a distribution of energy barriers and not only from the lowest one, it is not necessary, then, to have very aggressive approaches to block regions of the phase space. This is why standard KMC with kinetically correct flicker handling algorithms is as efficient as BEP methods with Tabu-like approaches for avoiding trapping.

5. CONCLUSION

In this paper, we use kinetic ART, an on-the-fly off-lattice kinetic Monte Carlo algorithm that incorporates exactly all elastic effects, to assess the role of the various elements of the recently proposed Bell–Evans–Polanyi (BEP)-based method. We did so by comparing BEP with KMC as both were coupled to various methods for handling flickering states and traps.

Testing these methods on two systems we find that, as would be expected, pure BEP simulations, even when handling low-energy flickering states, become trapped rapidly in relatively high-energy configurations, while KMC runs manage to find ever lower energy states (on the simulation time scale). It is possible to overcome BEP's limits by adding a Tabu criterion on the visited transition states, similarly to what was observed coupling Tabu to efficient searching algorithms.[24] Even a relatively short memory kernel, with 50 states, is sufficient to bring the efficiency of the BEP method on par with KMC, even though the correct kinetics is lost.

This comparison of various algorithms used for sampling energy landscape allows us to better understand the crucial *replenish and relax* steps, necessary to escape local energy minima in a complex system, confirming recent results[34] and helping to understand why and how the BEP-based method works. They also point to the primary importance of handling the exit from a local basin, a step that can be achieved through a number of approaches.

Better understanding of the workings of recently proposed minimization algorithm should help us develop more efficient minimization methods but also relate these more closely to the structure of complex systems' energy landscape itself, which remains the fundamental goal of all these methods.

ASSOCIATED CONTENT

Ⓢ Supporting Information

Details of KMC and BEP simulations with both basin and Tabu for ion-implanted silicon as well as specific results for the KMC and BEP simulations with the basin approach for this system are provided to support the discussion presented here. This includes a description of the simulations, the initial configurations (Figure 1), energy relaxation as a function of KMC step (Figure 2), distribution of selected energy barriers (Figure 3), and the asymmetry energy for the top 10% events (Figure 4) for the two sets of simulations. This material is available free of charge via the Internet at http://pubs.acs.org.

■ AUTHOR INFORMATION

Corresponding Authors
*E-mail: kokou.gawonou.ntsouaglo@umontreal.ca.
*E-mail: normand.mousseau@umontreal.ca.

Notes
The authors declare no competing financial interest.

■ ACKNOWLEDGMENTS

■ REFERENCES

(1) Wales, D. J. *Energy Landscapes: Applications to Clusters, Biomolecules and Glasses*; Cambridge University Press: 2003.
(2) Barkema, G.; Mousseau, N. *Phys. Rev. Lett.* **1996**, *77*, 4358–4361.
(3) Wales, D. J.; Doye, J. P. *J. Phys. Chem. A* **1997**, *101*, 5111–5116.
(4) Voter, A. F. *Phys. Rev. Lett.* **1997**, *78*, 3908.
(5) Goedecker, S. *J. Chem. Phys.* **2004**, *120*, 9911–9917.
(6) Béland, L. K.; Brommer, P.; El-Mellouhi, F.; Joly, J.-F.; Mousseau, N. *Phys. Rev. E* **2011**, *84*, 046704.
(7) Wales, D.; Scheraga, H. *Science* **1999**, *285*, 1368–1372.
(8) Rossi, G.; Ferrando, R. *J. Phys.: Condens. Matter* **2009**, *21*, 084208.
(9) Evans, M. G.; Polanyi, M. *Trans. Faraday Soc.* **1935**, *31*, 875–894.
(10) Bell, R. P. *Proc. R. Soc. London, Ser. A* **1936**, *154*, 414–429.
(11) Marcus, R. A. *J. Phys. Chem.* **1968**, *72*, 891–899.
(12) Roy, S.; Goedecker, S.; Hellmann, V. *Phys. Rev. B* **2008**, *77*, 056707.
(13) Kushima, A.; Lin, X.; Yip, S. *J. Phys.: Condens. Matter* **2009**, *21*, 504104.
(14) Bahar, I.; Rader, A. *Curr. Opin. Struct. Biol.* **2005**, *15*, 586–592.
(15) Jensen, F. *Introduction to computational chemistry*; Wiley: 1999.
(16) Novotny, M. A. *Phys. Rev. Lett.* **1995**, *74*, 1–5.
(17) Athènes, M.; Bellon, P.; Martin, G. *Philos. Mag. A* **1997**, *76*, 565–585.
(18) Puchala, B.; Falk, M. L.; Garikipati, K. *J. Chem. Phys.* **2010**, *132*, 134104.
(19) Fichthorn, K. A.; Lin, Y. *J. Chem. Phys.* **2013**, *138*, 164104.
(20) Cao, L.; Stoltz, G.; Lelièvre, T.; Marinica, M.-C.; Athènes, M. *J. Chem. Phys.* **2014**, *140*, 104108.
(21) Glover, F., Laguna, M. *Tabu Search*; Kluwer Academic Publishers: Boston, MA, 1997.
(22) Chubynsky, M. V.; Vocks, H.; Barkema, G. T.; Mousseau, N. *J. Non-Cryst. Solids* **2006**, *352*, 4424–4429.
(23) El-Mellouhi, F.; Mousseau, N.; Lewis, L. *Phys. Rev. B* **2008**, *78*, 153202.
(24) Grebner, C.; Becker, J.; Stepanenko, S.; Engels, B. *J. Comput. Chem.* **2011**, *32*, 2245–2253.
(25) Bortz, A. B.; Kalos, M.; Lebowitz, J. L. *J. Comput. Phys.* **1975**, *17*, 10–18.
(26) Fichthorn, K. A.; Weinberg, W. H. *J. Chem. Phys.* **1991**, *95*, 1090–1096.
(27) Joly, J.-F.; Béland, L. K.; Brommer, P.; El-Mellouhi, F.; Mousseau, N. *J. Phys. Conf. Ser.* **2012**, *341*, 012007.
(28) Mousseau, N.; Béland, L. K.; Brommer, P.; Joly, J.-F.; El-Mellouhi, F.; Machado-Charry, E.; Marinica, M.-C.; Pochet, P. *J. At., Mol., Opt. Phys.* **2012**, *2012*, 1–14.

(29) McKay, B. D. *Congr. Numer.* **1981**, *30*, 45−87.

(30) Malek, R.; Mousseau, N. *Phys. Rev. E* **2000**, *62*, 7723−8.

(31) Machado-Charry, E.; Béland, L. K.; Caliste, D.; Genovese, L.; Deutsch, T.; Mousseau, N.; Pochet, P. *J. Chem. Phys.* **2011**, *135*, 034102.

(32) Brommer, P.; Mousseau, N. *Phys. Rev. Lett.* **2012**, *108*, 219601.

(33) Béland, L. K.; Anahory, Y.; Smeets, D.; Guihard, M.; Brommer, P.; Joly, J.-F.; Pothier, J.-C.; Lewis, L. J.; Mousseau, N.; Schiettekatte, F. *Phys. Rev. Lett.* **2013**, *111*, 105502.

(34) Béland, L. K.; Mousseau, N. *Phys. Rev. B* **2013**, *88*, 214201.

(35) Brommer, P., Béland, L. K., Joly, J.-F., Mousseau, N. *Phys. Rev. B.* **2014**, *90*, 134109.

(36) Joly, J.-F.; Béland, L. K.; Brommer, P.; Mousseau, N. *Phys. Rev. B* **2013**, *87*, 144204.

(37) Ackland, G.; Mendelev, M.; Srolovitz, D.; Han, S.; Barashev, A. *J. Phys.: Condens. Matter* **2004**, *16*, S2629.

(38) Stillinger, F. H.; Weber, T. A. *Phys. Rev. B* **1985**, *31*, 5262.

(39) Xu, H.; Stoller, R. E.; Osetsky, Y. N. *J. Nucl. Mater.* **2013**, *443*, 66.

(40) Chill, S. T.; Henkelman, G. *J. Chem. Phys.* **2014**, *140*, 214110.

(41) Fan, Y.; Kushima, A.; Yip, S.; Yildiz, B. *Phys. Rev. Lett.* **2011**, *106*.

(42) Kallel, H.; Mousseau, N.; Schiettekatte, F. *Phys. Rev. Lett.* **2010**, *105*, 045503.

(43) Goedecker, S.; Hellmann, W.; Lenosky, T. *Phys. Rev. Lett.* **2005**, *95*, 055501.

(44) Kazachenko, S.; Thakkar, A. *J. Chem. Phys. Lett.* **2009**, *476*, 120−124.

(45) Sicher, M.; Mohr, S.; Goedecker, S. *J. Chem. Phys.* **2011**, *134*, 044106.